1N-34
33196
31P

NASA Contractor Report 194991

ICASE Report No. 94-83

ICASE

ON THE EVOLUTION OF CENTRIFUGAL INSTABILITIES WITHIN CURVED INCOMPRESSIBLE MIXING LAYERS

S. R. Otto
T. L. Jackson
F. Q. Hu

Contract NAS1-19480
October 1994

Institute for Computer Applications in Science and Engineering
NASA Langley Research Center
Hampton, VA 23681-0001

Operated by Universities Space Research Association

On the evolution of centrifugal instabilities within curved incompressible mixing layers

S. R. Otto[(1)] , T. L. Jackson[(2)] and F. Q. Hu[(3)]

[(1)] School of Mathematics and Statistics
The University of Birmingham, Edgbaston
Birmingham, B15 2TT, United Kingdom

[(2)] ICASE, Mail Stop 132 C
NASA Langley Research Center, Hampton
Virginia 23681–0001, USA

[(3)] Department of Mathematics and Statistics
Old Dominion University
Norfolk, Virginia 23529, USA

ABSTRACT

It is known that certain configurations which possess curvature are prone to a class of instabilities which their 'flat' counterparts will not support. The main thrust of the study of these centrifugal instabilities has concentrated on curved solid boundaries and their effect on the fluid motion. In this article attention is shifted towards a fluid–fluid interface observed within a curved incompressible mixing layer. Experimental evidence is available to support the conjecture that this situation may be subject to centrifugal instabilities. The evolution of modes with wavelengths comparable with the layer's thickness is considered and the high Taylor/Görtler number régime is also discussed which characterises the ultimate fate of the modes.

Research was supported by the National Aeronautics and Space Administration under NASA contract No. NAS1–19480 while the authors were in residence at the Institute for Computer Applications in Science and Engineering (ICASE), NASA Langley Research Center, Hampton, VA 23681-0001.

1 Introduction

The understanding of the dynamics involved in mixing layers is crucial in many physical problems. The necessarily inflectional profile can support inviscid modes which are known to be responsible for a great deal of the structures that are observed. The work of Michalke (1964,1965) describes the temporal and spatial linear stability of incompressible shear layers. The catalogue of work concerning this situation is immense; it suffices to say that the problem has been studied by many prolific authors. However, one physical process that has received relatively little attention is the subject tackled herein; that is, the effect of centreline curvature on the stability of curved mixing layers.

Most of the work to date concerning this particular subject has considered turbulent mixing layers, namely Margolis & Lumley (1965), Wyngaard, Tennekes, Lumley & Margolis (1968), Castro & Bradshaw (1976), Wang (1984), Karasso & Mungal (1990,1991), LeBoeuf (1991) and more recently Plesniak, Mehta & Johnston (1994). Two recent articles have tackled the problem analytically, concerning themselves with the fate of order one wavenumber vortices within highly curved situations. Liou (1994) is devoted to the effect of curvature on inflectional modes and also identifies three–dimensional steady centrifugal modes. Hu, Otto & Jackson (1994) (henceforth referred to as HOJ) is concerned both with that problem and also the question of the pure inviscid Görtler problem, given in Drazin & Reid (1979). We can summarize the findings of HOJ as follows: *(i)* the effect of centreline curvature on the Rayleigh modes appears to be minimal, and *(ii)* the presence of curvature permits an unstable three–dimensional mode which will become the prominent mode as the streamwise wavelength decreases (this corresponds to reverting to the centrifugal case for which this wavelength is zero). The apparent features of the inviscid Görtler problem can be described as when the centreline curves into the faster stream, the situation can support a family of unstable modes. However, if the centreline curves into the slower stream the situation is totally stable to inviscid Görtler modes.

Since the early work of Taylor (1923) and Görtler (1940) there has been a host of articles devoted to the study of centrifugal instabilities. Taylor (1923) demonstrates that the flow between two concentric cylinders is susceptible to toroidal modes when the inner cylinder rotates at an angular velocity with a value within a certain interval. In an exterior problem, namely the flow over a curved plate, Görtler showed the boundary layer on a concave plate will support longitudinal vortices. These modes remain within the boundary layer and have spanwise wavelengths comparable with the boundary layer thickness. It is known that the evolution of Görtler vortices is strongly dependent on their initial form and position, and the thickening of the boundary layer plays a critical role in their fate. It was in the work of Hall (1983) that the full parabolic linear Görtler equations were solved numerically. It was shown that it is essential for the layer's evolution to be included in the analysis. A starting condition was used which was consistent with the equations and the solution was progressed downstream. It was shown that the structure of the mode depended heavily on the streamwise position at which the disturbance was imposed. The characteristics of the modes, independent of initial form and position, eventually coalesce, so that the idea that one can exploit a far downstream asymptotic structure is an option. This involves considering high wavenumber vortices in a high Görtler number situation; this analysis was originally given in Hall (1982). The numerical techniques used here to solve the full problem are drawn from an article which considers the role of pressure gradients and crossflow in determining the structure of centrifugal modes, Otto & Denier (1994); slight modifications have been made to the techniques used in Hall (1983). The main aim of this article is to demonstrate that the curved mixing layer can support centrifugal modes for a finite downstream distance.

As hinted at previously, the consideration of high centrifugal parameter asymptotics can be very revealing. The high Taylor/ Görtler number régime is split into two distinct problems; firstly the inviscid modes and secondly the right hand branch modes. The former of these problems is pertinent when a mode with spanwise wavelength comparable with the boundary layer thickness is introduced into a high Taylor–Görtler number situation. The second problem occurs when a mode has a high wavenumber (ie short wavelength) and it attains a neutral state. As a layer thickens the centrifugal modes are known to maintain their wavelength, hence the local wavelength actually decreases. As the wavenumber of the modes increases in the inviscid problem we should match directly onto the small wavenumber limit of the righthand branch calculation. It is in this intermediate régime that the most unstable linear mode is encountered. In the Görtler problem this régime contains a large spike, due to the fact that the mode is driven to the wall where the basic velocity becomes zero (Denier, Hall & Seddougui (1991), henceforth referred to as DHS). In the current case the velocity is non–zero where the mode resides and hence we do not expect to find this significantly more dangerous mode.

In the conventional Görtler problem the basic state is uneffected by the situation's curvature and this is also true in our case. However, unlike the Görtler case in which the basic state is given by a Blasius profile, it is not clear which profile to use. As mentioned previously, the evolution of the layer is crucial and it is probably not sufficient to use the normal hyperbolic tangent profile, although it will be adequate in the high Görtler number case. Another possibility is the Lock profile (1951) in which the normal velocity is taken to be zero at the centreline. We shall present results for the order one problem using the Lock profile.

The remainder of this article is structured as follows: in section 2 we formulate the problem at hand, then in sections 3 and 4 we consider the high Görtler number problems and their subsequent matching. In section 5 the numerical methods used to solve the order one wavenumber problem are described in brief. In section 6 the results of the numerical calculations are given and finally in section 7 some conclusions are drawn.

2 Formulation

The problem considered here is the stability of an incompressible steady laminar mixing layer which lies between two streams with different speeds in a channel with curvature $\chi(x)$. A schematic is given in figure 1. The upper stream is travelling at U_0 and the lower stream travelling at $\beta_u U_0$. We assume that the Reynolds number $Re = U_0 d/\nu$ of the situation is large, where $d = R_2 - R_1$ is the height of the channel, assumed to be constant, and ν is the kinematic viscosity. Here, R_2 is the radius of the outer wall and R_1 is the radius of the inner. We consider the incompressible Navier-Stokes equations in cylindrical coordinates, such that the mixing layer lies along $r^* = R_1 + d/2 + dy^*$. The velocities are nondimensionalized by U_0 and lengths by d. We assume that the local curvature of the channel $\delta = d/R_1$ is small. The nondimensional steady equations, assuming $\delta << 1$, are thus given by

$$\frac{\partial u}{\partial x} + \frac{\partial v}{\partial y} + \frac{\partial w}{\partial z} = 0,$$

$$u\frac{\partial u}{\partial x} + v\frac{\partial u}{\partial y} + w\frac{\partial u}{\partial z} = -\frac{\partial p}{\partial x} + \frac{1}{Re}\nabla^2 u,$$

$$u\frac{\partial v}{\partial x} + v\frac{\partial v}{\partial y} + w\frac{\partial v}{\partial z} - \chi\delta u^2 = -\frac{\partial p}{\partial y} + \frac{1}{Re}\nabla^2 v,$$

$$u\frac{\partial w}{\partial x} + v\frac{\partial w}{\partial y} + w\frac{\partial w}{\partial z} = -\frac{\partial p}{\partial z} + \frac{1}{Re}\nabla^2 w,$$

where ∇^2 is the three dimensional Laplacian operator. We assume that the mixing layer is confined to a small region about $y = 0$, and hence rescale the velocity components (v, w) and coordinates (y, z) by $Re^{-1/2}$. This spanwise scaling is used since we know the vortices have wavelengths commensurate with the layer's thickness. We write the flow field as a sum of the mean flow and its perturbation

$$\mathbf{q} = \left(\bar{u}, Re^{-1/2}\bar{v}, 0, 1\right) + \Delta\left(\tilde{U}(x,y), Re^{-1/2}\tilde{V}(x,y), Re^{-1/2}\tilde{W}(x,y), Re^{-1}\tilde{P}(x,y)\right)e^{ikz},$$

where k is the wavenumber in the z direction. The parameter Δ is a vanishingly small so that the resulting analysis is linear and we may discard terms proportional to Δ^2.

We shall focus on two standard models for the mean flow. The first model is the Lock model, with the velocity components given by

$$\bar{u} = f'(\eta), \quad \bar{v} = \frac{1}{\sqrt{2x}}(\eta f' - f)$$

where

$$f''' + ff'' = 0, \qquad f'(\infty) = 1, \;\; f(0) = 0, \;\; f'(-\infty) = \beta_u,$$

and η is the similarity variable $y/\sqrt{2x}$. This model takes into account the non-parallel nature of the mean flow, necessary for the study of Görtler vorticies. The second model involves approximating the mean velocity profile by a hyperbolic tangent

$$\bar{u} = \frac{1}{2}\left(1 + \beta_u + (1 - \beta_u)\,\tanh\eta\right), \quad \bar{v} = 0.$$

We will call this approximation the Tanh model. Most of the results that will be presented below are for the Lock model, but we include some discussion for the Tanh model since it is a standard approximation to the mixing layer.

The perturbation equations are given by

$$\begin{aligned}\mathcal{L}\left(\frac{\partial^2}{\partial y^2} - k^2\right)\tilde{V} - G\chi k^2 \bar{u}\tilde{U} + 2\frac{\partial^2 \tilde{U}}{\partial x \partial y}\frac{\partial \bar{u}}{\partial x} + 2\frac{\partial \tilde{U}}{\partial x}\frac{\partial^2 \bar{u}}{\partial x \partial y} \\ + \tilde{U}\frac{\partial^3 \bar{u}}{\partial x^2 \partial y} + \frac{\partial \tilde{V}}{\partial x}\frac{\partial^2 \bar{u}}{\partial y^2} + \frac{\partial \tilde{V}}{\partial y}\frac{\partial^2 \bar{u}}{\partial x \partial y} + \tilde{V}\frac{\partial^3 \bar{u}}{\partial x \partial y^2} + \frac{\partial \bar{v}}{\partial x}\frac{\partial^2 \tilde{U}}{\partial y^2} + \\ - \frac{\partial \bar{v}}{\partial y}\frac{\partial^2 \tilde{V}}{\partial y^2} + k^2 \tilde{U}\frac{\partial \bar{v}}{\partial x} + k^2 \tilde{V}\frac{\partial \bar{v}}{\partial y} = 0\end{aligned} \tag{2.1a}$$

and

$$\mathcal{L}\left(\tilde{U}\right) = \frac{\partial \bar{u}}{\partial x}\tilde{U} + \frac{\partial \bar{u}}{\partial y}\tilde{V}, \tag{2.1b}$$

where the differential operator $\mathcal{L}$ is given by

$$\mathcal{L} \equiv \frac{\partial^2}{\partial y^2} - k^2 - \bar{u}\frac{\partial}{\partial x} - \bar{v}\frac{\partial}{\partial y}.$$

These equations have the opposite sign for the Görtler term when compared to the conventional Görtler problem due to the choice of the coordinate system. The Görtler number G is equal to $2\delta\sqrt{Re}$ and it is held fixed at an order one value as $Re \to \infty$ and $\delta \to 0$. We shall shortly consider the limit $G \to \infty$ (but still less than the square root of the Reynolds number). The appropriate boundary conditions are

$$\tilde{U}, \quad \tilde{V}, \quad \frac{\partial \tilde{V}}{\partial y} \quad \to 0 \;\text{ as }\; y \to \pm\infty. \tag{2.1c}$$

The numerical and asymptotic solution to the above system is considered in the following sections.

3 Viscous Right Hand Branch Modes

It is known that as a Görtler vortex progresses downstream it maintains its spanwise wavelength, and hence the local wavenumber, $kx^{\frac{1}{2}} = k_x$, increases. Also the local Görtler number, $G\chi x^{\frac{3}{2}} = G_x$ increases and hence it is pertinent to consider a high Görtler number calculation. As $G \to \infty$ it is known that $k \sim G^{\frac{1}{4}}$ (if $\chi \sim x^{\frac{1}{2}}$) near the righthand branch of the neutral curve. For simplicity we shall absorb the leading order curvature term χ_0 in the Görtler number. In this régime it is known that the mode becomes localised within a thin layer of thickness $k^{-\frac{1}{2}}$ situated at $\bar{y}$ say, Hall (1982). We introduce a layer variable and relevant disturbances quantities so that

$$y = \bar{y} + k^{-\frac{1}{2}}\psi, \qquad \tilde{U} = \left(\tilde{U}_0 + k^{-\frac{1}{2}}\tilde{U}_1 + \cdots\right)E, \qquad \text{and} \quad \tilde{V} = k^2\left(\tilde{V}_0 + k^{-\frac{1}{2}}\tilde{V}_1 + \cdots\right)E$$

where $E = \exp\left[k^2 \int \left(\beta_0 + k^{-\frac{1}{2}}\beta_1 + \cdots\right) dx\right]$ and again we are considering steady modes. Since we wish to move away from the neutral curve we also expand G in terms of k, so that

$$G = k^4\left[G_0 + k^{-\frac{1}{2}}G_1 + \cdots\right].$$

Substituting these forms into the governing equations and combining the streamwise and normal momentum equations at zeroth and first order, it is found that

$$\left(\bar{u}_0\beta_0 + 1\right)^2 + \bar{u}_0\bar{u}_1G_0 = 0 \tag{3.1}$$

and

$$2\beta_0\bar{u}_1\left(\beta_0\bar{u}_0 + 1\right) + G_0\left(\bar{u}_0\bar{u}_2 + \bar{u}_1^2\right) = 0, \tag{3.2}$$

where we have expanded $\bar{u}$ locally using a conventional Taylor series as

$$\bar{u} = \bar{u}_0(x) + k^{-\frac{1}{2}}\psi\bar{u}_1(x) + k^{-1}\frac{\psi^2}{2}\bar{u}_2(x) + \cdots.$$

The consistency conditions given by (3.1) and (3.2) provide the growth rate and location of the mode, namely β_0 and $\bar{y}$. Transforming these conditions to the similarity variables we have

$$\left(\beta^* f' + (\lambda^*)^2\right)^2 + f'f'' = 0, \tag{3.3}$$

and

$$2\beta^* f''\left(\beta^* f' + (\lambda^*)^2\right) + (f'f'')' = 0, \tag{3.4}$$

where $\lambda = G_0^{-\frac{1}{4}}$, with λ and β_0 scaled as

$$\beta_0 = \frac{\beta^*\sqrt{G_0}}{(2x)^{\frac{1}{4}}} \qquad \text{and} \qquad \lambda = \frac{\lambda^*}{(2x)^{\frac{1}{8}}}.$$

Note that since $f' = \bar{u}$ is positive thoughout the region the condition (3.1) (and hence (3.3)) requires that $f'' < 0$ at $\bar{\eta} = \bar{y}/(2x)^{\frac{1}{2}}$, that is $\bar{u}_y$ must be negative and the lower stream must be faster, hence $\beta_u > 1$ (the centreline curves into the faster stream). Figure 2 depicts the growth rate β^* versus λ^* for both the Tanh and Lock profiles with $\beta_u = 2$; it should be noted how close both models are. As $\lambda^* \to 0$, which corresponds to tending towards the inviscid régime, both models predict that β^* tends to a constant, 0.585786 for the Tanh model and 0.575432 for the Lock model. If we concern ourselves with the neutral mode, that is when $\beta^* = 0$, the location of the layer is given by the location at which $(f'f'')'$ is zero (see (3.4)) and λ^* can be found using the relationship

$$\lambda_N^* = (-f'f'')^{\frac{1}{4}}.$$

For the Tanh model with $\beta_u = 2$ we find that $\bar{\eta} = -0.16$ yielding $\lambda_N^* = 0.9367$ and for the Lock profile λ_N^* is essentially unaltered, however the layer location is now at $\bar{\eta} = -0.67$. In figure 3 we show the effect of changing β_u on $\bar{\eta}$ and λ_N^*. Although there is little difference in λ_N^* between the two models, the location of the modes are quite different. At next order the correction to the growth rate is given by

$$\beta_1 = -\frac{\bar{u}_1 G_1}{2\left(\bar{u}_0\beta_0 + 1\right)} = -\frac{\bar{u}_1 G_1 \lambda^4}{2\sqrt{-\bar{u}_0\bar{u}_1}},$$

which tends to zero as $\lambda \to 0$. At the next order the leading order eigenfunctions are determined, which satisfy a parabolic cylinder equation as is the case in the Görtler problem discussed in Hall (1982).

4 Inviscid modes

DHS have shown that the proper expansion of $\tilde{U}$ and $\tilde{V}$ as $G \to \infty$ with $k = O(1)$ is given by

$$\tilde{U} = e^{\sqrt{G}\int \beta dx}\left(U_0(x,y) + G^{-1/2}U_1(x,y) + \cdots\right),$$

$$\tilde{V} = \sqrt{G}e^{\sqrt{G}\int \beta dx}\left(V_0(x,y) + G^{-1/2}V_1(x,y) + \cdots\right),$$

where β is the growth rate in the streamwise direction. Substituting into the governing equations yields, at leading order, the system

$$\beta\bar{u}U_0 + \frac{\partial \bar{u}}{\partial y}V_0 = 0, \qquad \beta(\frac{\partial^2 \bar{u}}{\partial y^2} - \bar{u}\frac{\partial^2}{\partial y^2} + k^2\bar{u})V_0 - k^2\bar{u}U_0 = 0.$$

This system can be rewritten by eliminating U_0, yielding

$$-\beta^2\bar{u}(\frac{\partial^2}{\partial y^2} - k^2 - \frac{1}{\bar{u}}\frac{\partial^2 \bar{u}}{\partial y^2})V_0 = -k^2\frac{\partial \bar{u}}{\partial y}V_0.$$

The appropriate boundary conditions are $V_0 \to 0$ as $y \to \pm\infty$, which corresponds to the mode being confined to the layer. Since $\bar{u}$ is given in terms of the similarity variable η, it is convenient to transform the above equation, resulting in

$$-\beta^{*^2} f'(\frac{\partial^2}{\partial \eta^2} - k^{*^2} - \frac{f'''}{f'})V_0 = -k^{*^2} f'' V_0, \tag{4.1}$$

where

$$k = \frac{k^*}{\sqrt{2x}}, \quad \beta = \frac{\beta^*}{(2x)^{1/4}}.$$

The above equation was solved numerically for the Tanh model only, using a fourth order Runge-Kutta technique, shooting in from $\eta = \pm\infty$ and matching the function and its derivative at $\eta = 0$. These results were checked using a fourth order finite difference scheme. A stretched grid was used to reduce the number of points needed to retain sufficient accuracy. The results presented henceforth in this section are given for the case $\beta_u = 2$, in which the mixing layer curves into the fast stream. It was found, as was to be expected, that for values of β_u less than unity there were no unstable vortex modes. The spatial growth rates for the first four modes are given in figure 4, and the eigenforms of these modes are given in figure 5. Upon comparing the unstable mode of the right hand branch shown in figure 2 and the unstable modes of the inviscid regime shown in figure 4, we see that the growth rate plateaus between the inviscid regime and right hand branch of the neutral curve. This mimics the Taylor problem in which, at leading order, the most unstable mode is not well defined. On the other hand, in the Görtler problem there is a class of modes with distinctly higher growth rates within this regime, as identified by DHS. We have thus verified that the mixing layer must curve into the faster stream in order to be unstable to longitudinal inviscid centrifugal instabilities. This is equivalent to the concave curvature condition for Görtler vortices.

We now show that the inviscid solutions in the limit $k^* \to \infty$ matches with the viscous right hand branch solutions as $\lambda^* \to 0$. We begin by first plotting in figure 6 the inviscid eigenfunctions V_0 for the Tanh model verses η for three wavenumbers $k^* = 3.5$, $k^* = 26$ and $k^* = 100$. Note that as k^* increases, the structure shrinks to a thin layer, consistent with the asymptotic solution for the right branch. To begin the matching process, we first set $k^* = \epsilon^{-1}$ and take the limit $\epsilon \to 0$. Let η_b be the location of the mode, and set

$$\eta = \eta_b + \delta\xi$$

where $\delta = \delta(\epsilon)$. We now expand the quantities

$$\beta^* = \beta_0 + \delta\beta_1 + \delta^2\beta_2 + \cdots, \qquad f = f_b + \delta\xi f_b' + \frac{1}{2}\delta^2\xi^2 f_b'' + \cdots.$$

Substitution into the equation (4.1) yields the conditions,

$$\beta_1 = 0, \qquad f''' f' - (f'')^2 = 0 \ \text{ at } \ \eta = \eta_b.$$

The first condition shows that as $k^* \to \infty$ the growth rate tends to a constant value (see figure 4), whilst the second condition defines the location of the layer (this is shown in figure 6 as a vertical dashed line). The eigenfunction satisfies a parabolic cylinder equation which matches with the viscous right branch provided the choices $\epsilon = G^{-1/4}$ and $\delta = O(\sqrt{\epsilon})$ are made.

5 Numerical Methods used to solve (2.1)

The governing equations are parabolic, and thus are solved using a marching procedure in the downstream direction. This makes the whole process orders of magnitude less expensive that the corresponding elliptic problem. The numerical methods used here are taken from Otto & Denier (1994), with slight modifications to cope with the infinite range (rather than the semi–infinite domain used in that problem). The equations are discretized in the downstream coordinate using a Crank–Nicholson scheme, and a standard second order finite difference technique is used in the normal coordinate. This yields a coupled penta-diagonal and tri-diagonal system which is inverted using techniques detailed in Otto & Bassom (1993). The entire system is then inverted using a fairly complicated Thomas algorithm, which serves to retain more of the nature of the system, and hence makes the scheme slightly more implicit than if the penta and tri systems are solved individually. In order to resolve the detail at the centreline, an algebraically stretched grid is used in the normal coordinate, with outer limits at $\pm 40\,(x)^{\frac{1}{2}}$. We chose to solve the problem using the similarity variables, and thus the grid naturally spreads to resolve the layer.

An initial condition was imposed at a streamwise location, $\bar{x}$ say, of the form

$$\tilde{U} = \left(\mathcal{U} + (\eta - \tilde{\eta})^2\right) e^{-(\eta-\tilde{\eta})^2}, \qquad \tilde{V} = 0 \tag{5.1}$$

where $\tilde{\eta}$ in some sense is the centre of the imposed disturbance and $\mathcal{U}$ is another free parameter. As one would expect the modes were found to change with $\tilde{\eta}$, but the characteristics coalesced downstream as predicted in Hall (1982) and observed in Hall (1983). Results are also presented for the initial condition given by

$$\tilde{U} = (\eta - \tilde{\eta})^3\, e^{-(\eta-\tilde{\eta})^2}, \qquad \tilde{V} = 0. \tag{5.2}$$

The essential difference is that the modes are now odd functions of η about $\tilde{\eta}$. As the modes progress downstream we monitor the evolution using the energy measure in physical space

$$\mathcal{E}(x) = \int_{\eta=-\infty}^{\eta=\infty} \tilde{U}^2 d\eta = \frac{1}{\sqrt{2x}} \int_{y=-\infty}^{y=\infty} \tilde{U}^2 dy$$

and define the spatial growth rate as

$$\sigma(x) = \frac{\mathcal{E}_x}{\mathcal{E}} + \frac{1}{2x}.$$

We are largely interested in determining the location where the modes start to grow. Since in a real problem some distance downstream of this location it is likely that nonlinear effects will come into play. Hence we shall produce neutral curves of G_x versus k_x (both defined in section 3), where a neutral point is defined as where the real part of σ changes sign (in this case σ is always real; if we were to consider temporal oscillations to the problem this would result in less unstable modes, as shown in Otto & Denier (1994)).

The basic state is taken to be the Lock model and is generated using a fourth order Runge–Kutta scheme in conjunction with a two–dimensional secant method. The mean flow quantities are constructed from the similarity forms at each station rather than marching the boundary layer equations forward. We shall now discuss the results of our calculations.

6 Results

In this section we present results concerning Görtler modes with wavelengths commensurate with the mixing layer's thickness and for order one Görtler numbers. It is clear that there are no local approximations which can deal with this problem other than predicting the far downstream behaviour. The majority of 'local' approximations use the argument that since the flow evolves over longer scales in the streamwise coordinate than in the normal layer variable, the streamwise derivative of $\bar{u}$, and hence $\bar{v}$, is zero (from continuity). This argument allows one to use a normal mode analysis, with $\tilde{U} = \hat{U}e^{i\alpha x}$, where α is the eigenvalue. Whilst this is suitable for the inviscid modes in which the streamwise evolution is on a far shorter scale than the boundary layer evolves on, it is not so in the Görtler problem.

In some parallel flow work instabilities are actually predicted with zero spanwise wavenumber. In Otto & Denier (1994) a favourable pressure gradient was found to destabilize Görtler vortices which is in direct contradiction to the conclusion reached by Ragab & Nayfeh (1980) using parallel arguments. In Otto & Denier (1994) it was found that as the pressure gradient increased, the right hand branch of the neutral curve moved to the right (as it does with an increase in β_u here). The marching calculations were able to reproduce this behaviour. We shall include similar comparisons here.

We solved equation (2.1) subject to the initial conditions (5.1) with $\mathcal{U} = 5$ and $\tilde{\eta} = 5$.

Note that the disturbance was placed above the centreline. Similar results were obtained for the cases $\tilde{\eta} = 0$ and $\tilde{\eta} = -5$ and will not be presented here. The curvature is taken to have the form $\chi = \sqrt{x/\bar{x}}$ and the Görtler number was taken to be $G = 1/20$. In figure 7 we plot G_x versus k_x for $\beta_u = 10$, $6\frac{2}{3}$, 2.5 and 2. Note that as β_u increases (i.e. greater disparity between the freestream speeds), the right hand branch moves to the right, consistent with the analysis presented in section 3. Also note that as the value of β_u increases, the minimum of G_x decreases. This is found to be true for other initial conditions. Here, as in Hall (1983) and Otto & Denier (1994), the centre and left hand parts of the neutral curve are dependent on the particular initial conditions chosen. For comparison, we also show in figure 7 results using the odd initial conditions (5.2) with $\beta_u = 2$. In figure 8 we plot the growth rate $\sigma(x)$ as a function of x for the initial condition (5.1) with $\mathcal{U} = 5$, $\tilde{\eta} = 5$ and $\beta_u = 10$ (dashed curve) and $\beta_u = 2$ (solid curve). In each case, the wavenumber k chosen corresponds to its respective minimum shown in figure 7; for $\beta_u = 10$, $k = 0.071$ and for $\beta_u = 2$, $k = 0.053$. Note that the mode corresponding to the case $\beta_u = 10$ becomes unstable earlier and has a larger growth rate than the case for $\beta_u = 2$. This is consistent with experimental observations that as the speed of the fast stream increases, the flow becomes more unstable.

To illustrate the streamwise structure of the Görtler modes, we plot in figure 9 the spanwise vorticity

$$\begin{aligned} \omega_z &= -u_y + v_x \\ &= -\bar{u}_y + \bar{v}_x + \Delta\left(-\tilde{U}_y + \tilde{V}_x\right) e^{ikz} + \cdots \end{aligned}$$

at various downstream locations and with $\Delta = 0.002$. The initial conditions and parametric values are the same as in figure 8 for $\beta_u = 2$. Note that as the downstream distance increases, streamwise vortices emerge and appear to "ride" on top of the centreline. Although these streamwise vortices will produce large scale structures, they may not be an efficient mechanism for mixing enhancement since they are predominant on one side of the mixing layer and are confined within.

We remark here that the choices of $\mathcal{U}$ and $\tilde{\eta}$ are in a sense arbitrary since the starting condition is artificial and is not derived from any rigorous analysis. In this paper we merely wish to demonstrate that the curved mixing layer can support centrifugal instabilities. We are not trying to identify the most unstable mode. It is our intention to provide information concerning the receptivity of this situation in the near future. In the article of Hall (1990) the problem of freestream receptivity of Görtler vortices within a boundary layer was considered and, by using similar techniques, we intend to demonstrate the receptivity of the situation considered herein to freestream disturbances.

In figure 10 we plot the neutral curves for the case $G = -1/20$, $\beta_u = 2$ and $\chi = \sqrt{x/\bar{x}}$ (solid) and $\chi = 1$ (dashed). The initial condition used in these calculations was taken to be (5.1) with $\tilde{\eta} = 0$ and $\mathcal{U} = 5$. The negative Görtler number corresponds to the case for which the centreline curves into the slower stream. Note the somewhat surprising result of the existence of an unstable band for small spanwise wavenumbers. For wavenumbers larger than a critical value, the flow is stable for all Görtler numbers. This is consistent with the analysis presented in sections 3 and 4, as well as the recent work by Liou (1994) and HOJ.

Thus, all the high Görtler number modes are stable except for those in the neighbourhood of the left hand branch. We are not suggesting that these modes will be observed in a physical problem, merely that it is important to include all the physics of a problem since these modes would be missed by the parallel flow approximations. In figure 11 we show the energy $\mathcal{E}$ associated with these modes for the case $\chi = \sqrt{x/\bar{x}}$ and for several wavenumbers. As k decreases the modes become more unstable, suggesting that the most linearly unstable mode will have a very long spanwise wavelength. It would be interesting to explore the analysis of Choudhari, Hall & Streett (1994) for this problem. In that article the receptivity of long wavelength modes is discussed and the modes were found to operate within a triple deck type structure. The other information that can be gleaned from figure 11 is that the energy does not return its original value. This is probably the reason that these modes have not been reported in the experimental literature.

7 Concluding Remarks

In this paper we have demonstrated that the curved incompressible mixing layer can support centrifugal instabilities. As far as we are aware this is the first work which investigates the evolution of modes in curved mixing layers where the wavelengths are comparable with the layer's thickness and order one Görtler number situations. The extra parameters that this incurs make a parametric study enormous. However, we have shown that by solving the equations (2.1) we could predict a given mode's characteristics. In addition, we have shown that as the modes develop downstream, they conform to a far downstream asymptotic structure. It is in this régime that the parallel flow approximation could be used, however it is then irrelevant. We were also able to show that as β_u increased, the right hand branch moved to the right. This was shown using the asymptotic techniques of section 3 (refer to figure 3) and by direct solution of the full equations (2.1) (refer to figure 7).

In section 3 it was shown that as k decreased from its $O(G^{\frac{1}{4}})$ value the growth rate of the modes tended to a constant multiplied by $G^{\frac{1}{2}}$. Similarly in section 4 we showed that as k increased in the inviscid régime, the growth rate asymptoted to the same value. Thus, there is a direct matching between the two problems and the most unstable mode is not uniquely defined (at least to leading order). It is, however, still possible to identify the most unstable linear mode in these cases and the interested reader is referred to Otto & Bassom (1994) for a discussion of the Taylor case.

The surprising result of this article is that we were able to demonstrate that the case in which the centreline curved into the slower stream can also support centrifugal instabilities. It should be stressed that these modes grow for far reduced streamwise distances and do not seem to grow beyond their initial amplitudes (refer to figure 11) and thus are unlikely to be seen within experimental configurations. However, we have shown that the most unstable modes have very small wavenumbers, and their receptivity may be important, Choudhari, Hall & Streett (1994). This result does not contradict the work of Liou (1994) and HOJ, nor the analysis presented in sections 3 and 4, since we still predict that the inviscid and right hand branch modes are stable.

There is also the question of how curvature effects the growth of the Kelvin–Helmholtz instability. In HOJ, a size of curvature was used that was sufficient to allow centrifugal vortices to be obtained, whilst not effecting the Kelvin–Helmholtz modes. In Liou (1994), however, it was found that if the layer curved into the faster stream, not only were vortices produced but the inviscid modes also became more unstable. In HOJ, although the effect of the curvature on the two–dimensional modes was minimal, the most severe change was to the modes with short streamwise wavelengths, which would actually be close to the Görtler modes (which correspond to α_r zero). The reason given for the apparent insensitivity of the Kelvin–Helmholtz modes to the curvature was that they evolve over far shorter distances $O(R_e^{-\frac{1}{2}})$ than the centrifugal instabilities, $O(G^{-\frac{1}{2}})$ (one should recall that $G << R_e^{\frac{1}{2}}$). It is shown in HOJ that the most unstable temporal mode for small α in a slightly curved situation is in fact three–dimensional, which shows again the importance of vortical disturbances in curved mixing layers.

References

Castro, I. P. & Bradshaw, P. (1976) The turbulence structure of a highly curved mixing layer *J. Fluid Mech.* **73** 265

Choudhari, M., Hall, P. & Streett, C. L. (1994) On the spatial evolution of long–wavelength Görtler vortices governed by a viscous–inviscid interaction, Part 1: The linear case *QJMAM* **47** 207

Denier, J. P., Hall, P. & Seddougui, S. (1991) On the receptivity problem for Görtler vortices: vortex motion induced by wall roughness *Phil. Trans. Roy. Soc. Lond. A* **335** 51 (herein referred to as DHS)

Drazin, P.G. & Reid, W.H. (1979) Hydrodynamic Instability *Cambridge University Press*

Görtler, H. (1940) On the three dimensional instability of laminar boundary layers on concave walls *NACA Tech. Memo no. 1375*

Hall, P. (1982) Taylor–Görtler vortices in fully developed or boundary layer flows. *J. Fluid Mech.* **124** 475

Hall, P. (1983) The linear development of Görtler vortices in growing boundary layers. *J. Fluid Mech.* **130** 597

Hall, P. (1990) Görtler vortices in growing boundary layers: the leading edge receptivity problem, linear growth and the nonlinear breakdown stage *Mathematika* **37** 151

Hu, F. Q., Otto, S. R. & Jackson, T. L. (1994) On the Stability of a Curved Mixing Layer *in the proceedings of the ICASE workshop on Transition, Turbulence and Combustion, 1993, Kluwer, Editors: T. B. Gatski, M. Y. Hussaini & T. L. Jackson* (herein referred to as HOJ)

Karasso, P. S. & Mungal, M. G. (1990) An experimental study of curved mixing layers: flow visualization using volume rendering *Center for Turbulence, Annual Research Briefs* **195**

Karasso, P. S. & Mungal, M. G. (1991) Mixing measurements of straight and curved shear layers *Center for Turbulence, Annual Research Briefs* **343**

LeBoeuf, R. L. (1991) Progress toward identification of streamwise vorticity meander in a plane mixing layer *Center for Turbulence, Annual Research Briefs* **349**

Lock, R. C. (1951) The velocity distribution in the laminar boundary layer between parallel streams *Quart. J. Mech.* **4** 42

Liou, W. W. (1994) Linear Instability of curved free shear layers *Phys. Fluids* **6(2)** 541

Margolis, D. P. & Lumley, J. L. (1965) Curved Turbulent Mixing Layer *Phys. Fluids* **8** 1775

Michalke, A. (1964) On the inviscid instability of the hyperbolic-tangent velocity profile *J. Fluid Mech.* **19** 543

Michalke, A. (1965) On spatially growing disturbances in an inviscid shear layer *J. Fluid Mech.* **23** 521

Otto, S. R. & Bassom, A. P. (1993) An Algorithm for Solving the Viscous Equations Arising in the Stability of Three-Dimensional Centrifugal Instabilities *ICASE Internal Report, 38*

Otto, S. R. & Bassom, A. P. (1994) The effect of crossflow on Taylor vortices *QJMAM* **47** 323

Otto, S. R. & Denier, J. P. (1994) The Effect of Pressure Gradients and Three–Dimensional Flows on Görtler Vortices *submitted to J. Fluid Mech*

Plesniak, M. W., Mehta, R. D. & Johnston, J. P. (1994) Curved two–stream turbulent mixing layers: three–dimensional structure and streamwise evolution *J. Fluid Mech* **270** 1

Ragab, S. A. & Nayfeh, A. H. (1980) Effect of pressure gradients on Gortler instability *AIAA-80-1377*

Taylor, G.I. (1923) Stability of a viscous liquid contained between two rotating cylinders *Phil. Trans. R. Soc. Lond. A* **223** 289

Wang, C. (1984) The effects of curvature on turbulent mixing layers, PhD. thesis, California Institute of Technology

Wyngaard, J. C., Tennekes, H., Lumley, J. L. & Margolis, D. P. (1968) Structure of turbulence in a curved mixing layer *Phys. Fluids* **11(6)** 1251

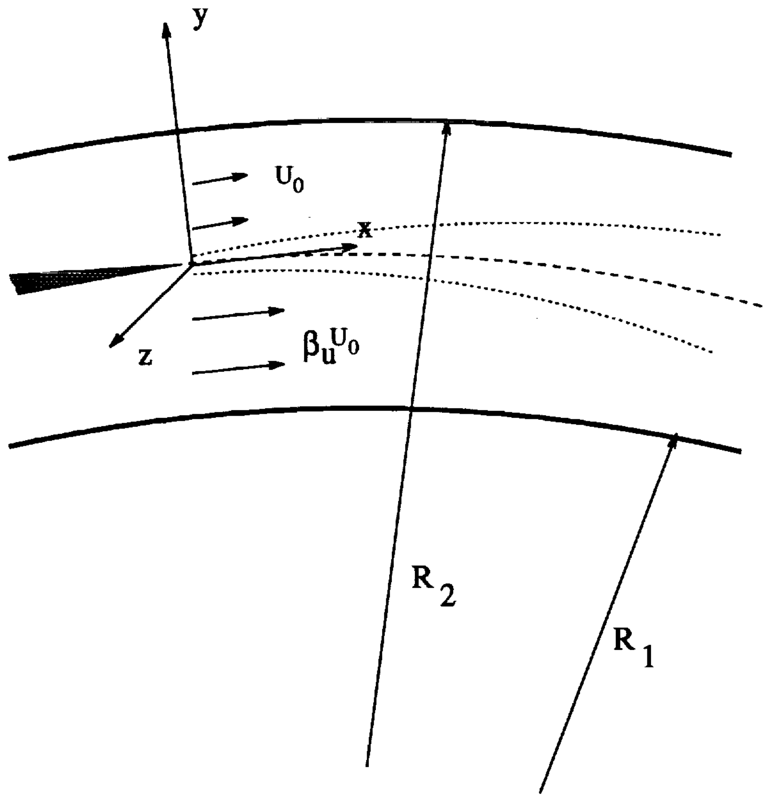

Figure 1: Schematic of flow

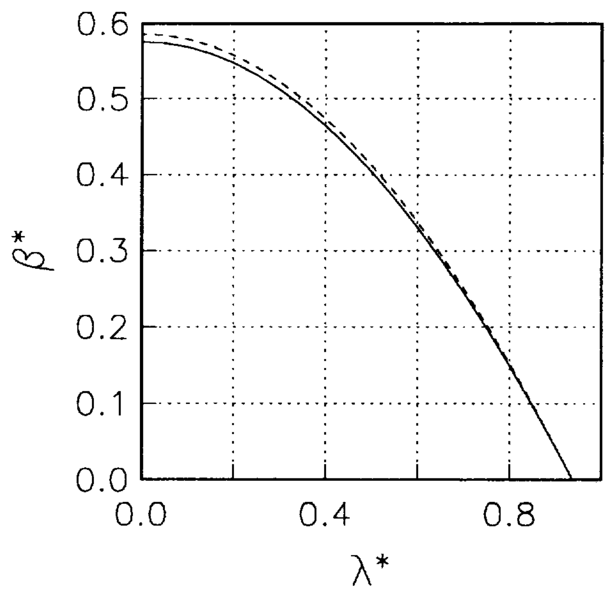

Figure 2: Variation of the scaled growth rate β^* with the scaled wavenumber λ^* with $\beta_u = 2$ (solid–Lock, dashed–Tanh)

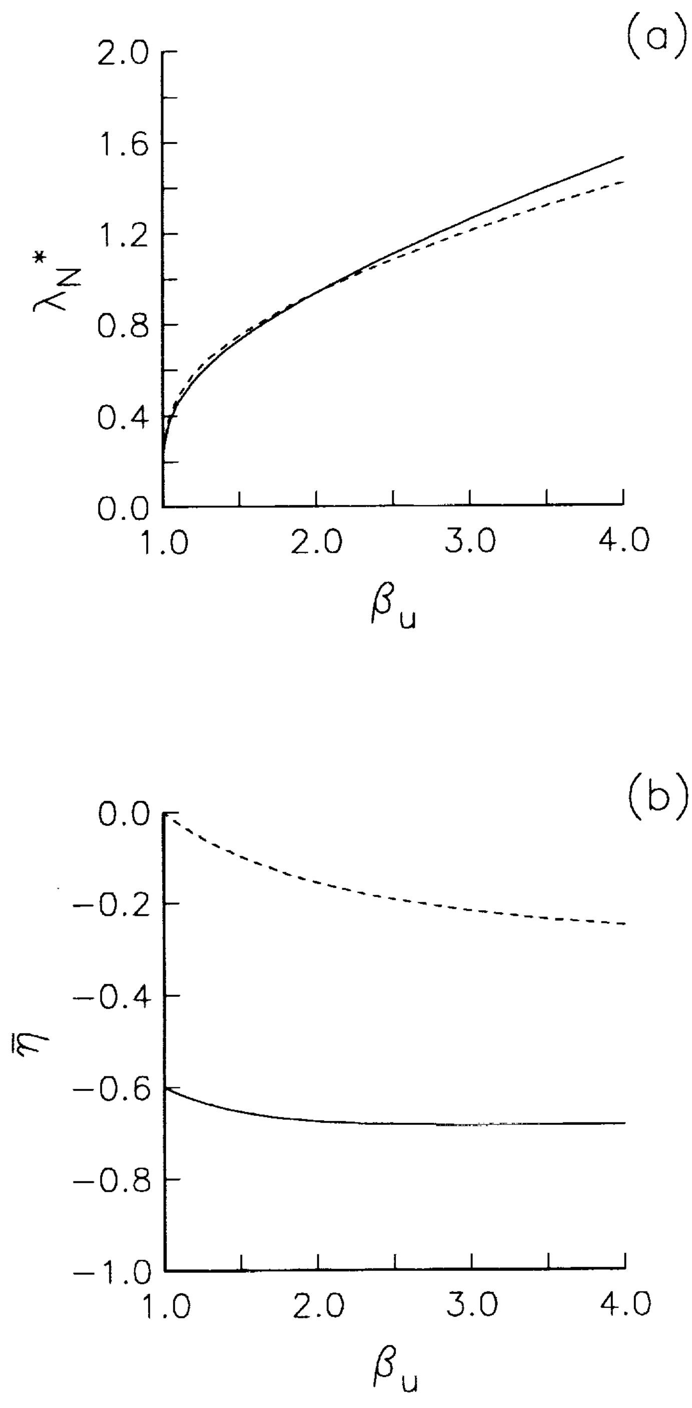

Figure 3(a) Variation of λ_N^* with β_u and

Figure 3(b) Variation of $\bar{\eta}$ with β_u (solid–Lock, dashed–Tanh)

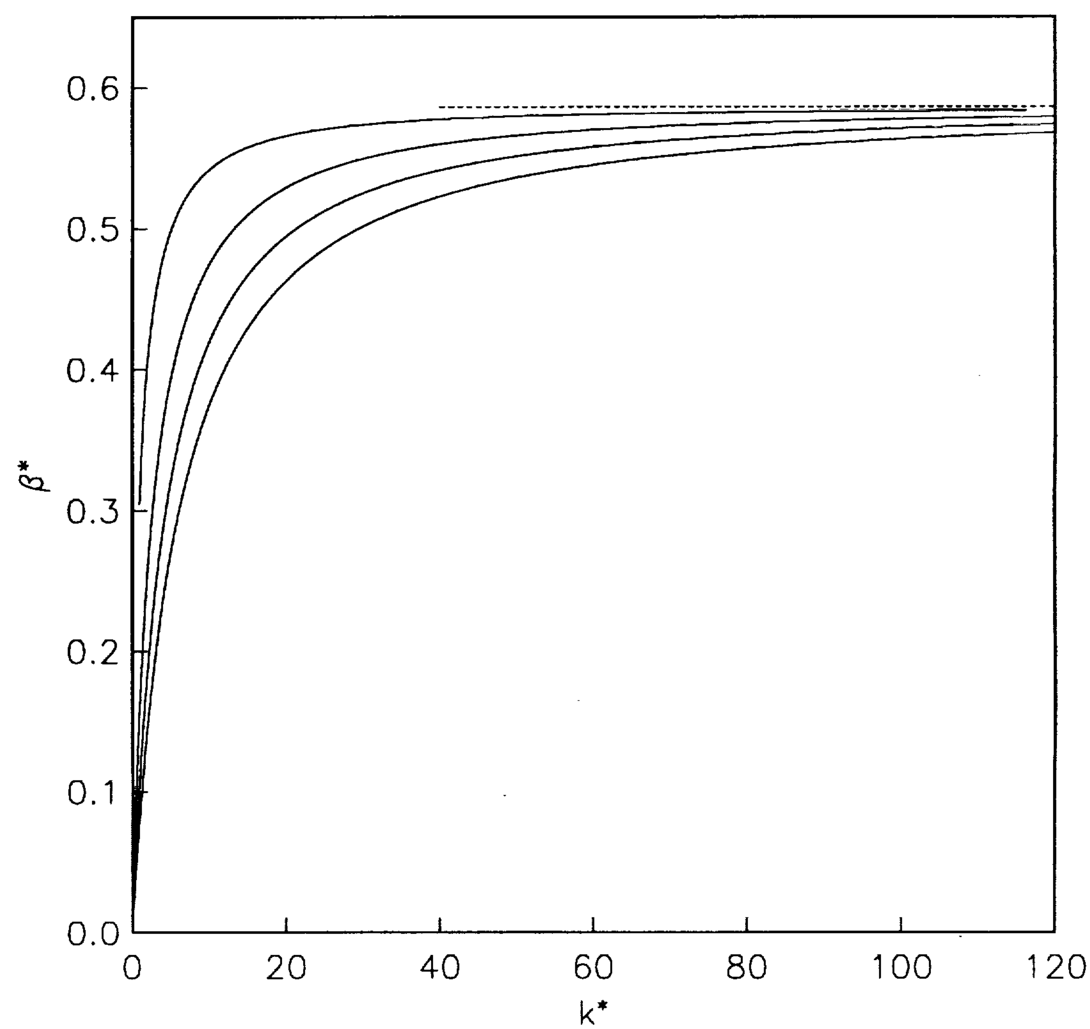

Figure 4: Inviscid growth rates for the first four modes with $\beta_u = 2$ and for the Tanh model (asymptote shown as dashed line)

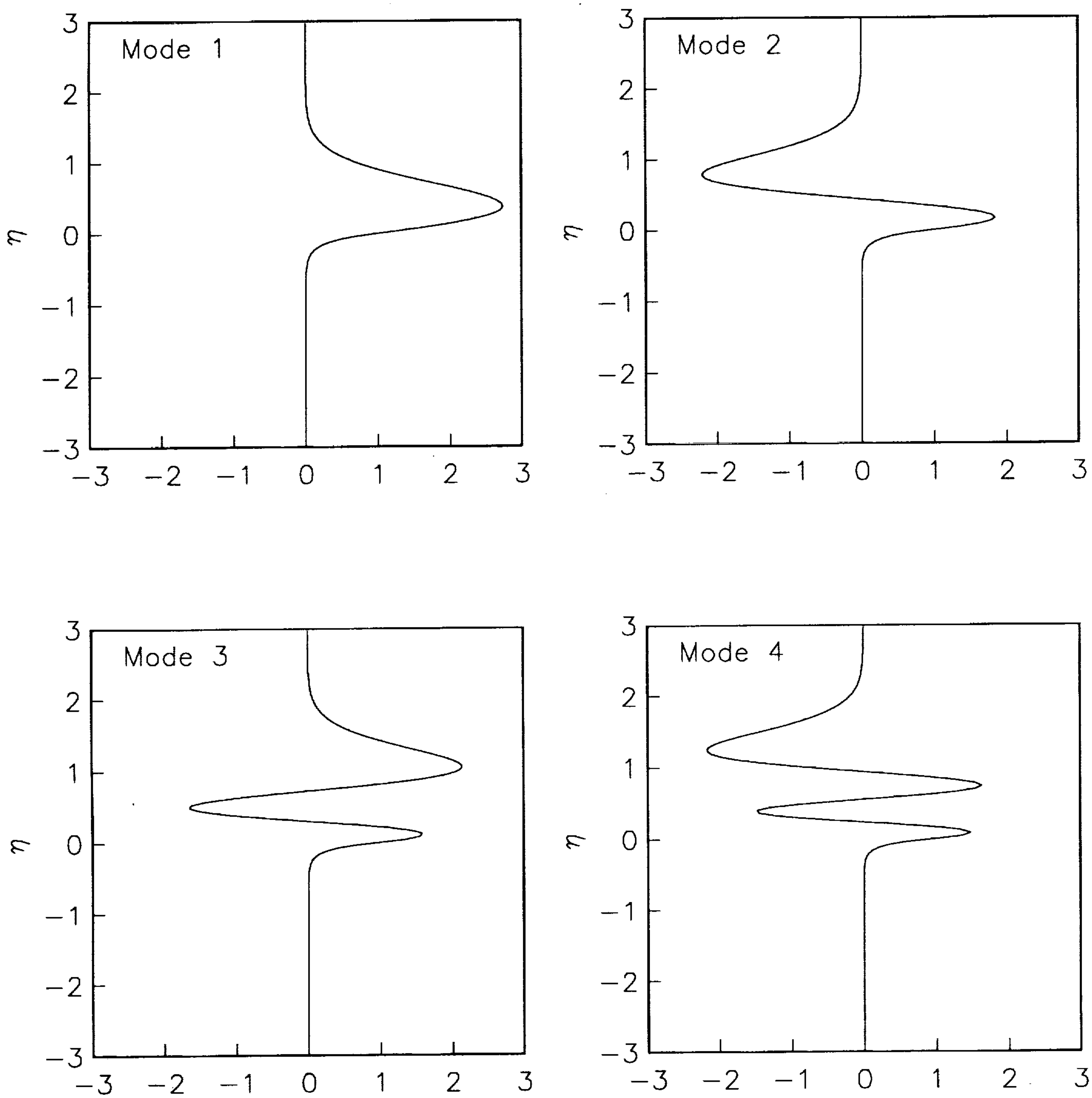

Figure 5: Eigenmodes for the first four inviscid modes with $\beta_u = 2$ and for the Tanh model (with $k^* = 6$)

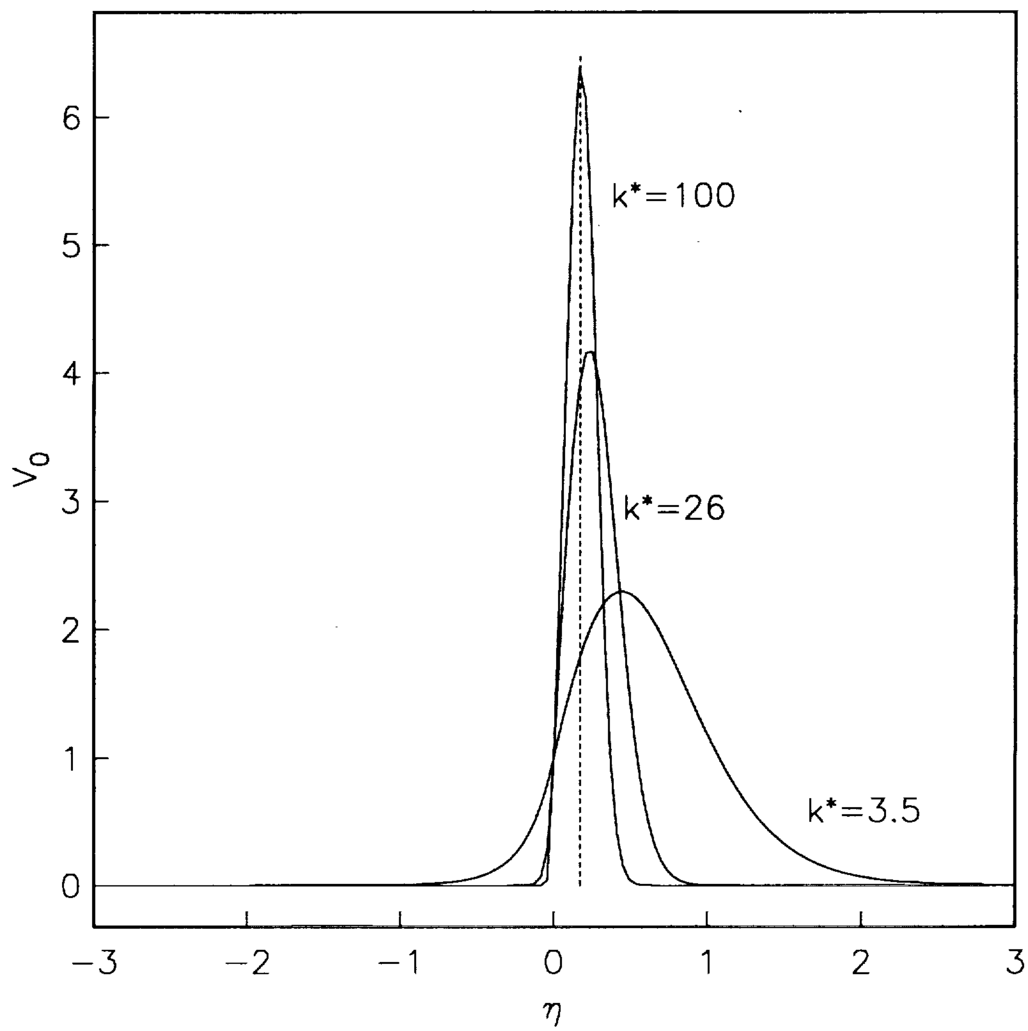

Figure 6: First inviscid modes for $k^* = 3.5$, $k^* = 26$ and $k^* = 100$ (theoretical location of vortex shown as vertical dashed line)

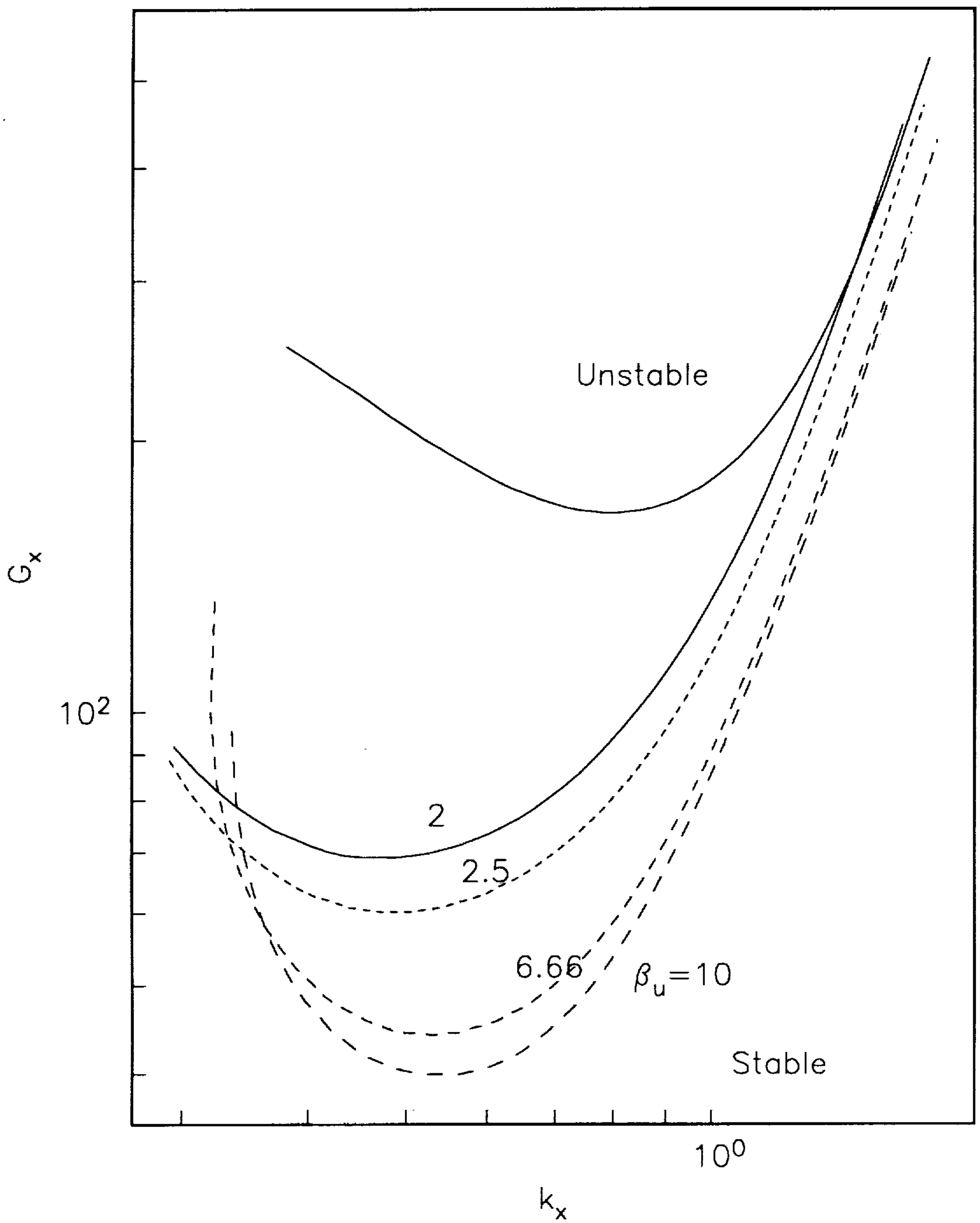

Figure 7: Neutral curves for $G = 1/20$, $\chi = \sqrt{x/\bar{x}}$, initial conditions (5.1), $\beta_u = 10$, $6\frac{2}{3}$, 2.5 and 2 ($\beta_u = 10$ lowest) and initial conditions (5.2) with $\beta_u = 2$ (upper solid curve).

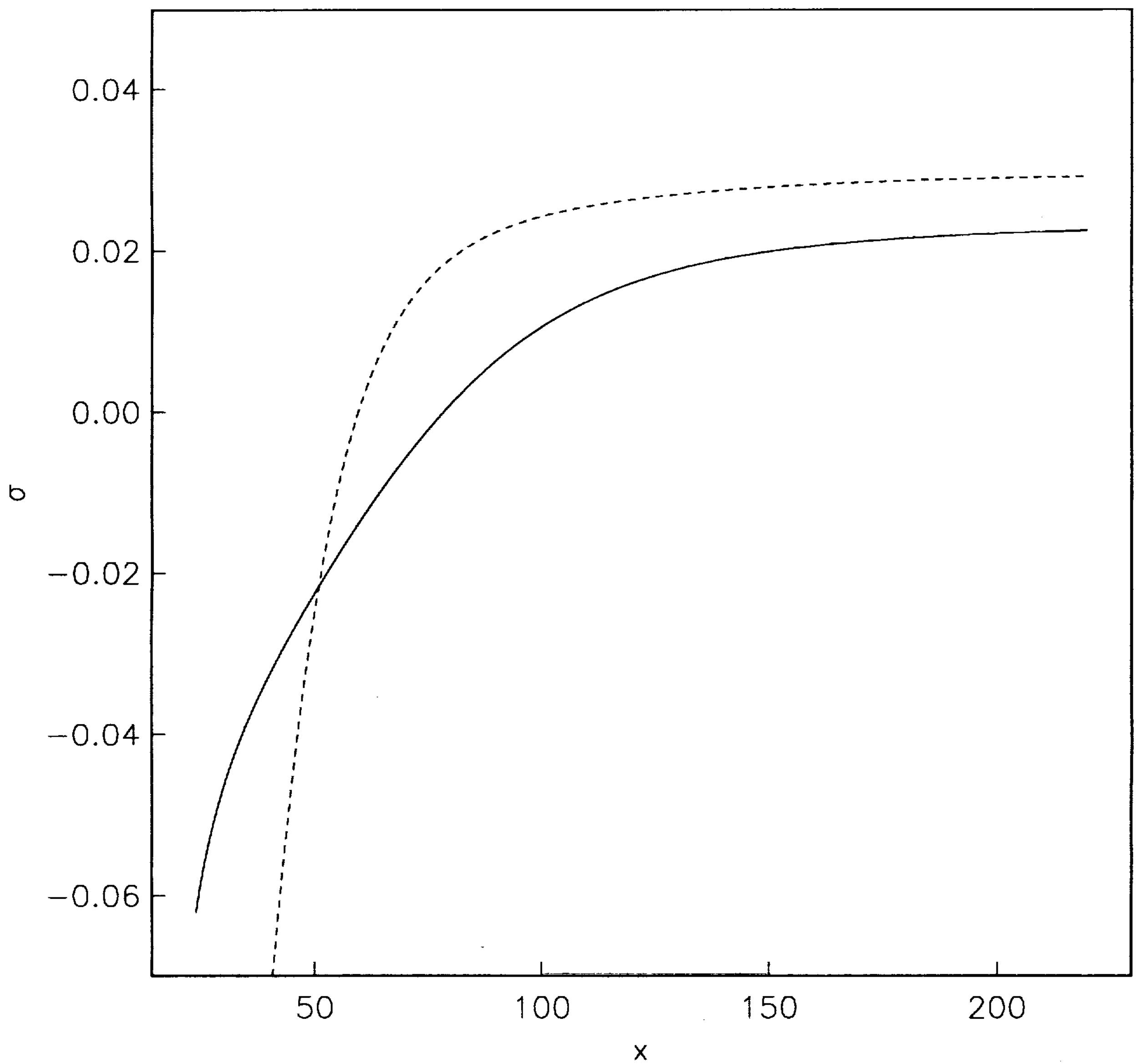

Figure 8: Growth rates for $\beta_u = 10$ (dashed) and $\beta_u = 2$ (solid) optimized for k

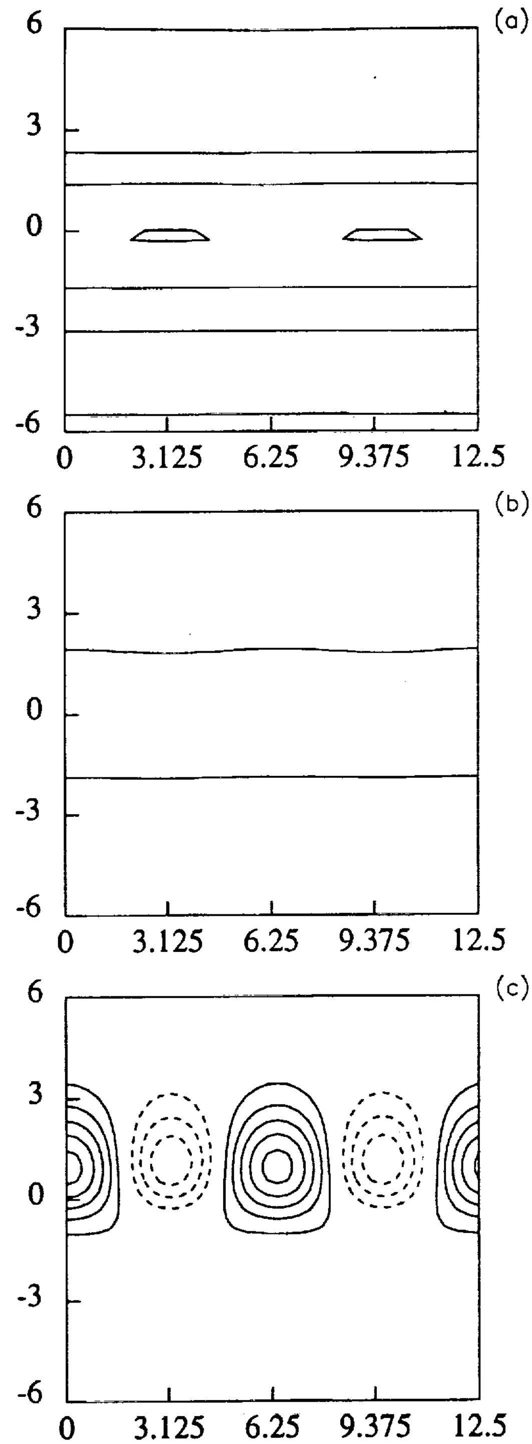

Figure 9: Spanwise vorticity at various downstream locations

(a) $x = 65.15$, (b) $x = 170.15$ and (c) $x = 590.15$.

Here, the initial condition was taken to be (5.1), with

$G = 1/20$, $\chi = \sqrt{x/\bar{x}}$, and $\beta_u = 2$.

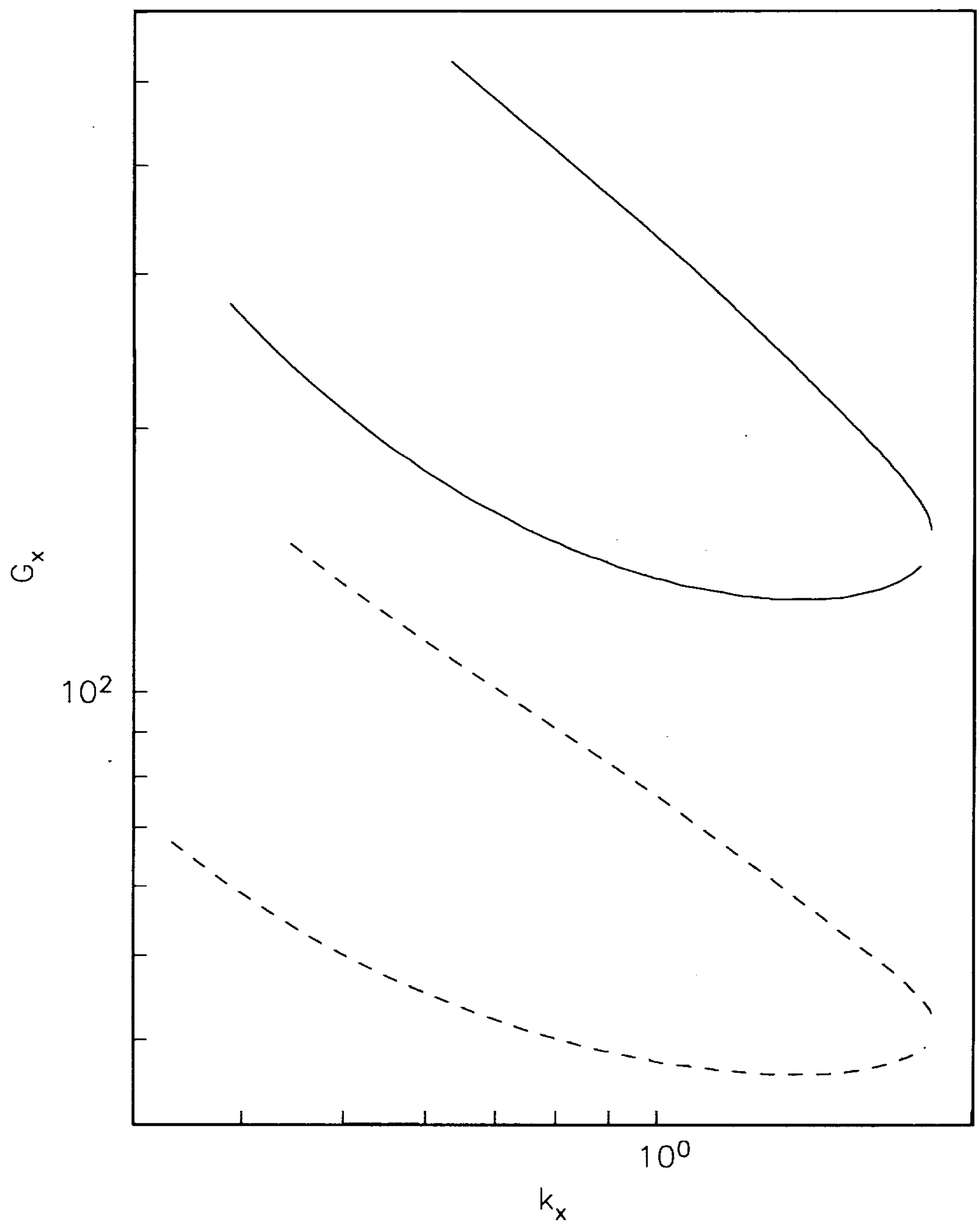

Figure 10: Neutral curves for $G = -1/20$ $\chi = \sqrt{x/\bar{x}}$ (solid) and $\chi = 1$ (dashed).

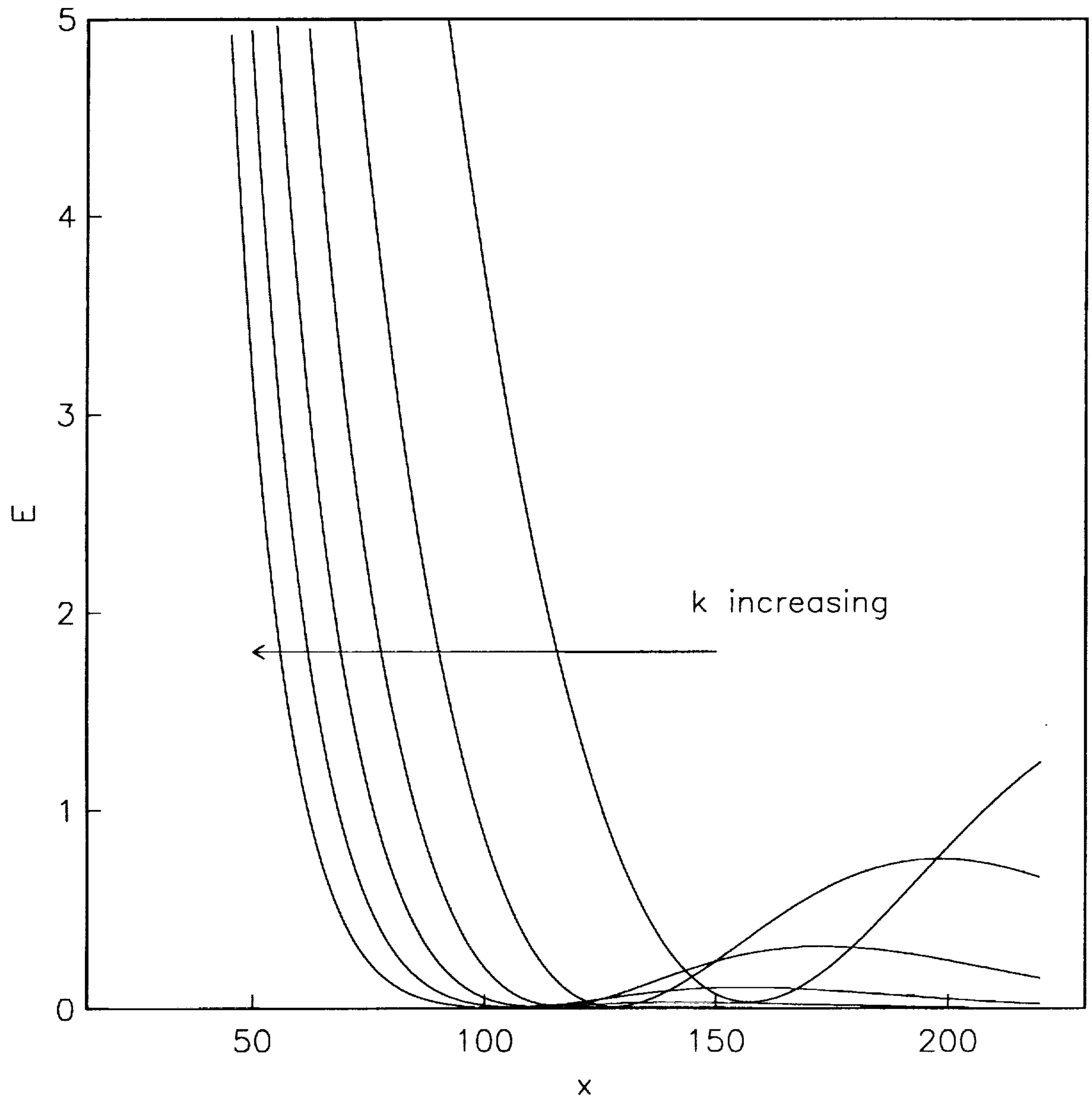

Figure 11: Energy $\mathcal{E}$ for $G = -1/20$ $\chi = \sqrt{x/\bar{x}}$

for $k = 0.031, 0.036, 0.041, 0.046, 0.051$ and 0.056

REPORT DOCUMENTATION PAGE

Form Approved
OMB No. 0704-0188

1. AGENCY USE ONLY *(Leave blank)*

2. REPORT DATE
October 1994

3. REPORT TYPE AND DATES COVERED
Contractor Report

4. TITLE AND SUBTITLE
ON THE EVOLUTION OF CENTRIFUGAL INSTABILITIES WITHIN CURVED INCOMPRESSIBLE MIXING LAYERS

5. FUNDING NUMBERS
C NAS1-19480
WU 505-90-52-01

6. AUTHOR(S)
S.R. Otto
T.L. Jackson
F.Q. Hu

7. PERFORMING ORGANIZATION NAME(S) AND ADDRESS(ES)
Institute for Computer Applications in Science and Engineering
Mail Stop 132C, NASA Langley Research Center
Hampton, VA 23681-0001

8. PERFORMING ORGANIZATION REPORT NUMBER
ICASE Report No. 94-83

9. SPONSORING/MONITORING AGENCY NAME(S) AND ADDRESS(ES)
National Aeronautics and Space Administration
Langley Research Center
Hampton, VA 23681-0001

10. SPONSORING/MONITORING AGENCY REPORT NUMBER
NASA CR-194991
ICASE Report No. 94-83

11. SUPPLEMENTARY NOTES
Langley Technical Monitor: Michael F. Card
Final Report
Submitted to Journal of Fluid Mechanics

12a. DISTRIBUTION/AVAILABILITY STATEMENT
Unclassified–Unlimited
Subject Category 34

12b. DISTRIBUTION CODE

13. ABSTRACT *(Maximum 200 words)*

It is known that certain configurations which possess curvature are prone to a class of instabilities which their 'flat' counterparts will not support. The main thrust of the study of these centrifugal instabilitie s has concentrated on curved solid boundaries and their effect on the fluid motion. In this article attention is shifted towards a fluid–fluid interface observed within a curved incompressible mixing layer. Experimental evi dence is available to support the conjecture that this situation may be subject to centrifugal instabilities. The evolution of modes with wavelengths comparable wi th the layer's thickness is considered and the high Taylor/Görtler number régime is also discussed which characterises the ultimate fate of the modes.

14. SUBJECT TERMS
curved mixing layer, centrifugal instability

15. NUMBER OF PAGES
30

16. PRICE CODE
A03

17. SECURITY CLASSIFICATION OF REPORT	18. SECURITY CLASSIFICATION OF THIS PAGE	19. SECURITY CLASSIFICATION OF ABSTRACT	20. LIMITATION OF ABSTRACT
Unclassified	Unclassified		